

# Infrared Absorption Spectroscopy of Small Carbon–Sulfur Clusters Isolated in Solid Ar

Jan Szczepanski, Robert Hodyss, Jason Fuller, and Martin Vala\*<sup>†</sup>

Department of Chemistry and Center for Chemical Physics, University of Florida, Gainesville, Florida 32611

Received: December 10, 1998; In Final Form: February 19, 1999

Small asymmetric and symmetric carbon–sulfur clusters,  $C_nS$  and  $SC_nS$  ( $n = 1–5$ ), have been generated by pulsed laser ablation of a carbon/sulfur mixture, deposited in an argon matrix at 12 K, and studied via Fourier transform infrared absorption spectroscopy. Previous vibrational band assignments for a number of these clusters have been confirmed and new assignments for others have been made using a combination of isotopic ( $^{12}C/^{13}C$ ) substitution and density functional (B3LYP/6-311G\*) and ab initio (MP2) theoretical calculations. Reactions of neutral  $C_n$  ( $n = 1–9$ ) and  $C_mS$  ( $m = 6–0$ ) fragments are shown theoretically to be highly exothermic. Evidence for such aggregation reactions in the formation of the clusters is found from isotopomeric band intensities. Given their calculated vibrational band intensities and estimated column densities, it is proposed that the direct observation via IR spectroscopy of  $C_5S$  and  $SC_5S$  clusters in the envelope of the carbon star, IRC+10216, and, possibly, the Taurus molecular cloud, TMC-1, is an attractive possibility.

## I. Introduction

Small clusters containing carbon and sulfur are attractive objects for spectroscopic study due to their involvement in interstellar chemistry and material science. The small CS,  $C_2S$ , and  $C_3S$  clusters, which possess large permanent dipole moments, have been identified by Cernicharo et al.<sup>1</sup> and by Yamamoto et al.<sup>2</sup> in the envelope surrounding the carbon star IRC+10216 and in the Taurus cold molecular dense cloud TMC-1 via radio telescopic observations. A tentative detection of  $C_5S$  in IRC+10216 by Bell et al. has also been reported.<sup>3</sup> The  $SC_nS$  clusters, having no or near-zero permanent dipole moments, have to date gone undetected because they are silent in radio astronomy observations.

The abundance of carbon sulfur clusters near interstellar objects is thought to be only slightly less than the corresponding pure carbon clusters. The column density for  $C_nS$  ( $n \leq 5$ ) clusters in the envelope of IRC+10216 is estimated to be  $4 \times 10^{13} \text{ cm}^{-2}$  (or higher), only slightly lower than the  $10^{14} \text{ cm}^{-2}$  estimation for the analogous  $C_n$  ( $n \leq 5$ ) pure carbon clusters.<sup>3</sup> In the realm of material science, amorphous organic semiconductor films, possibly containing  $C_nS_m$  species, exhibit unusual electrical properties. They show a dramatic resistance drop at particular applied voltages.<sup>4</sup>

Laboratory investigations of a number of carbon–sulfur clusters have been carried out. Maier and his group generated the carbon–sulfur clusters CS,  $C_3S$ ,  $C_2S_2$ ,  $C_3S_2$ ,  $C_4S_2$ , and  $C_5S_2$  by UV photolysis and flash pyrolysis of cyclic precursors containing C and S atoms and identified the cluster species by infrared absorption studies in Ar matrices.<sup>5–8</sup> Andrews and co-workers investigated the linear  $C_2S_2$  and  $C_3S_2$  clusters in Ar matrices by trapping the high-voltage discharge products of a  $CS_2/Ar$  mixture.<sup>9</sup> The species isolated were identified by infrared spectroscopy of the isotopically labeled analogues. Ohshima et al.,<sup>10</sup> Hirahara et al.,<sup>11</sup> and Kasai et al.<sup>12</sup> generated  $C_nS$  ( $n = 2–5$ ) clusters in the discharge of a gaseous  $C_2H_2/CS_2/Ar$  mixture and used Fourier transform microwave (FT-MW) spectrometry to determine their structures. Schwarz and co-workers observed

the  $C_nS_2$  ( $n = 2–6$ ) clusters using neutralization–reionization mass spectrometry.<sup>13</sup> Theoretical works on  $C_nS$  clusters have been carried out by a number of groups,<sup>14–20</sup> with earlier work being done on the smaller species ( $n = 2, 3$ )<sup>14–18</sup> and later work on the larger ones ( $n = 4–9$ ).<sup>19,20</sup> Seeger, Flugge, and Botschwina have reported<sup>19</sup> extensive ab initio work on  $C_3S$  and  $C_5S$ , while Lee has presented<sup>20</sup> density functional calculations on the linear polycarbon sulfide series,  $C_nS$  ( $n = 2–9$ ).

The present work is focused on the small carbon–sulfur clusters,  $C_nS_m$  ( $n = 1–5$ ,  $m = 1, 2$ ). The clusters were generated by laser ablation of a carbon and sulfur mixture. Infrared spectroscopic techniques using species with  $^{12}C/^{13}C$  isotopic substitution, aided by ab initio and density functional theory calculations of vibrational frequencies and intensities, have led to the identification of a number of carbon–sulfur clusters and the unambiguous assignment of a number of infrared transitions associated with them. The isotopic vibrational frequency shifts calculated at MP2/6-31G\* and B3LYP/6-311G\* levels of theory for  $^{12/13}C_nS_m$  ( $n = 1–5$ ,  $m = 1, 2$ ) clusters have been compared to the experimental isotopic frequency shifts. From this comparison, the geometry, size, and cluster type have been deduced.

## II. Experimental Section

Carbon–sulfur clusters were produced by the vaporization of pressed pellets of  $^{12}C$ ,  $^{13}C$ , and S in natural abundance (96%  $^{32}S$  and 4%  $^{34}S$ ) using a pulsed Q-switched Nd:YAG laser (1064/532 nm). The gaseous reaction products were mixed with Ar gas and trapped on a CsI window cooled to 12 K by a closed-cycle helium cryostat (ADP Displex). Reaction products were probably also formed on the surface of the matrix during landing of the carbon–sulfur material as well as during annealing of the matrix (to 36 K). Absorption spectra of the sample-containing matrices were recorded using a Nicolet Magna 560 Fourier transform infrared spectrometer in the 7000–700  $\text{cm}^{-1}$  region (with 0.25  $\text{cm}^{-1}$  resolution).

## III. Results and Discussion

**a. Calculations.** A number of ab initio and density functional theory (DFT) methods have previously been applied to the

<sup>†</sup> E-mail: mvala@chem.ufl.edu.

**TABLE 1: Optimized Bond Lengths (Å) at the B3LYP/6-311G\* Level of Theory for Linear  $SC_n$  ( $n = 1-5$ ) and  $SC_nS$  ( $n = 1-5$ ) Clusters in Their Electronic Ground States, and Bond Lengths for  $SC_nS$  (in Parentheses)**

bond	$n = 1$	$n = 2$	$n = 3$	$n = 4$	$n = 5$
S-C1	1.541 <sup>a</sup> (1.5603)	1.5751 <sup>b</sup> (1.5805)	1.5462 <sup>c</sup> (1.5626)	1.5676 (1.5751)	1.5541 (1.5648)
C1-C2		1.3141 <sup>b</sup> (1.2731)	1.2904 <sup>c</sup> (1.2738)	1.2751 (1.2717)	1.2798 (1.2735)
C2-C3			1.2789 <sup>c</sup> (1.2738)	1.2899 (1.2860)	1.2657 (1.2754)
C3-C4				1.2991 (1.2717)	1.2916 (1.2754)
C4-C5					1.2810 (1.2735)

<sup>a</sup> Experimental value,  $r_{S-C1} = 1.5348$  Å from ref 26. <sup>b</sup> Experimental bond lengths for  $SC_2$  are  $r_{S-C1} = 1.5669$  and  $r_{C1-C2} = 1.3101$  Å from ref 24. <sup>c</sup> Experimental  $r_{S-C1} = 1.5323$ ,  $r_{C1-C2} = 1.3028$ , and  $r_{C2-C3} = 1.2724$  Å for  $SC_3$  cluster from ref 10. The recommended mixed experimental/theoretical equilibrium structure from ref 18 is  $r_{S-C1} = 1.5363$ ,  $r_{C1-C2} = 1.2936$ , and  $r_{C2-C3} = 1.2800$  Å.

calculation of  $C_nS$  ( $n = 1-5$ ) cluster properties.<sup>14-20</sup> The DFT approach using the B3LYP functional with a 6-311G\* basis set (B3LYP/6-311G\*) was used here because of its proven reliability in the prediction of geometry, frequencies, and relative intensities. Full geometry optimization calculations were carried out for the  $C_nS$  and  $SC_nS$  ( $n = 1-5$ ) clusters with DFT programs from the GAUSSIAN 94 package.<sup>21</sup> Linear structures are predicted for all clusters. Table 1 shows the calculated bond lengths and a comparison with known experimental values.

Though primarily cumulenic in bond character, Table 1 shows that the  $C_nS$  ( $n > 2$ ) chains have a slight alternation in the C-C bond lengths in contrast to the  $C_nS_2$  ( $n > 2$ ) chains which exhibit "pure" cumulenic bonds. For example, the C2-C3 bond in  $C_5S$  is shorter by 0.0259 Å than the C3-C4 bond. It is also shorter by 0.0097 Å than the C2-C3 bond in  $C_5S_2$ . A Mulliken charge analysis from the B3LYP/6-311G\* results also shows some alternation in the charge distribution along the C-C chain in  $C_nS$  clusters. The negative charge is delocalized more uniformly over the CC framework of the  $SC_nS$  cluster chain than in the asymmetric  $C_nS$  clusters. In both  $C_nS$  and  $SC_nS$  clusters, the partial positive charge is located on the S atoms.

Carbon and carbon-sulfur clusters are known to aggregate and form larger clusters during matrix annealing (vide infra). It was therefore of interest to determine theoretically the energies of the reaction:  $C_nS$  ( $n = 0-6$ ) +  $C_m$  ( $m = 1-9$ ) →  $C_{n+m}S$  ( $n + m < 9$ ). The reaction energies were estimated by subtracting the sum of the total energies of the reactants from the total energy of the  $C_{n+m}S$  product. Zero-point energy corrections (usually 5% or less of the total energy) were not included in the reaction energies. Figure 1 shows that all the reaction energies predicted here are highly exothermic. They range from -85 kcal/mol for CS +  $C_3$  to -205 kcal/mol for  $C_2S$  +  $C_2$ . Generally, the aggregation reactions between carbon-sulfur clusters and even-membered carbon clusters are found to be 10-30% more exothermic than reaction energies between carbon-sulfur clusters and odd-membered carbon clusters (Figure 1). This is in contrast to the reaction energies between a sulfur atom and carbon clusters where no odd-even alternation with carbon chain size is predicted, just a simple asymptotic increase with cluster size to -120 kcal/mol.

Calculated harmonic vibrational frequencies (unscaled), integrated intensities, rotational constants, and dipole moments of the  $C_nS_m$  ( $n = 1-5, m = 1,2$ ) clusters are presented in Table 2. For the asymmetric  $C_nS$  clusters, all modes are infrared active. The most intense C-C vibrations of  $C_nS$  and  $C_nS_2$  have

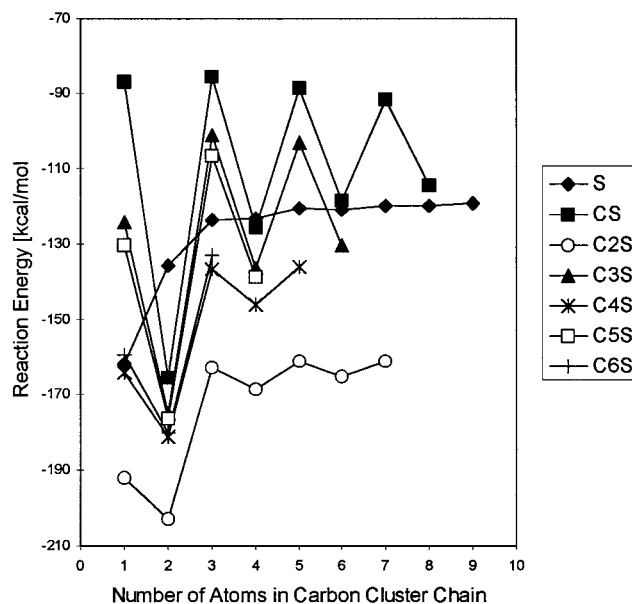


**Figure 1.** Calculated (B3LYP/6-311G\*) reaction energies between the linear  $C_n$  ( $n = 1-9$ ) carbon clusters and the linear  $C_nS$  ( $n = 0-6$ ) carbon-sulfur clusters in their electronic ground states.

intensities which are generally higher than the analogous  $C_n$  carbon clusters, calculated at the same level of theory. For example, the most intense band in the  $C_3S_2$  cluster is twice as intense as that in the  $C_3S$  cluster and over 4 times as intense as the similar mode in  $C_3$ . From a comparison of the calculated frequencies (scaled to one experimental frequency, cf. Table 3), we can conclude that vibrational frequency predictions are quite reasonable with a maximum 18  $cm^{-1}$  discrepancy for the  $C_4S$  cluster in the  $C_nS$  series. For  $SC_nS$  clusters, the worst prediction is off 22  $cm^{-1}$  for the  $SC_3S$  and  $SC_4S$  clusters. It should be stressed that all C-C and C-S vibrational frequencies were scaled uniformly by a common scaling factor for each type of vibration. The relative intensities calculated here are also in concert with experimental values. It is, however, difficult to estimate accurate absolute IR intensities. For example, for  $C_3S$  Seeger et al.<sup>18</sup> using the CCSD(T) method predict 1431.1 km/mol for the  $\nu_1$  mode intensity, a value thought to be accurate to ca. 5%. The 1529 km/mol intensity value calculated using B3LYP/6-311G\* (Table 2) falls just outside the 5% uncertainty range (1503-1360 km/mol) recommended by Seeger et al.<sup>18</sup>

**b. Experimental Infrared Spectra.** Infrared absorption spectra of the laser ablated products of a carbon and sulfur mixture trapped in solid Ar at 12 K are presented in Figure 2. Assignments of bands to pure carbon clusters (marked) are based on earlier work summarized in the recent review article by Orden and Saykally.<sup>23</sup> Several bands due to small  $C_nS$  and  $C_nS_2$  clusters were previously observed in matrices by Maier<sup>5-8</sup> and Andrews.<sup>9</sup> The IR absorption spectra of larger carbon-sulfur clusters will be discussed in a future publication.

**$C_3S$  Cluster.** The 2047.6  $cm^{-1}$  band (in Ar) was previously assigned by Maier, Schrot, Reisenauer, and Janoschek<sup>5</sup> to  $C_3S$ . The complete isotopomeric spectrum of the  $^{12}C_3^{32}S$  cluster has, however, not yet been reported. In Figure 3, we present the absorption spectrum (in the 2080-1960  $cm^{-1}$  region) of an ablated  $^{12}C_3^{32}S$  mixture. Almost all bands in this region are due to well-known isotopomers of  $^{12}C_3^{23}S$  and  $^{12}C_3^{32}S_2$ .<sup>9</sup> A set of eight new bands built on the 2047.6  $cm^{-1}$  band (and marked with \*) are assigned here to  $^{12}C_3^{32}S$  isotopomers. Comparison of the observed and calculated (MP2/6-31G\* and B3LYP/6-311G\*) isotopic shifts is shown in Table 4. Generally, the deviation between the calculated and experimental values

**TABLE 2: Vibrational Harmonic Frequencies (Unscaled,  $\text{cm}^{-1}$ ), IR Intensities (in Brackets,  $\text{km/mol}$ ), Symmetries, Rotational Constants ( $B_e$ , GHz), and Electric Dipole Moments ( $\mu$ , debye) for Linear Carbon–Sulfur Clusters  $\text{C}_n\text{S}$  ( $n = 1-5$ ) and  $\text{SC}_n\text{S}$  ( $n = 1-5$ ) in Their Electronic Ground States (Calculated at the B3LYP/6-311G\* Level)**

$\text{CS}(\Sigma^+)$	1301 [87] $\sigma$ ; $B_e = 25.7430$ ; $\mu = 1.84$
$\text{C}_2\text{S}(\Sigma^-)$	1721 [42] $\sigma$ , 860 [14] $\sigma$ , 266 [2 $\times$ 7] $\pi$ ; $B_e = 6.4241$ ; $\mu = 2.88$
$\text{C}_3\text{S}(\Sigma^+)^b$	2145 [1529] $\sigma$ , 1567 [67] $\sigma$ , 739 [14] $\sigma$ , 480 [2 $\times$ 0.2] $\pi$ , 160 [2 $\times$ 3] $\pi$ ; $B_e = 2.8798$ ; $\mu = 3.50^b$
$\text{C}_4\text{S}(\Sigma^-)$	2118 [30] $\sigma$ , 1810 [537] $\sigma$ , 1223 [5] $\sigma$ , 612 [7] $\sigma$ , 408 [2 $\times$ 0.002] $\pi$ , 311 [2 $\times$ 6] $\pi$ , 127 [2 $\times$ 5] $\pi$ ; $B_e = 1.5140$ ; $\mu = 4.03$
$\text{C}_5\text{S}(\Sigma^+)^d$	2240 [3997] $\sigma$ , 2088 [0.2] $\sigma$ , 1656 [618] $\sigma$ , 1091 [79] $\sigma$ , 543 [7] $\sigma$ , 496 [2 $\times$ 6] $\pi$ , 411 [2 $\times$ 2] $\pi$ , 211 [2 $\times$ 6] $\pi$ , 76 [2 $\times$ 2] $\pi$ ; $B_e = 0.9209$ ; $\mu = 4.65$
$\text{SCS}(\Sigma_g^+)$	1572 [649] $\sigma_u$ , 680 [0] $\sigma_g$ , 401 [2 $\times$ 0.9] $\pi_u$ ; $B_e = 3.2463$ ; $\mu = 0.01$
$\text{SC}_2\text{S}(\Sigma_g^-)$	1982 [0] $\sigma_g$ , 1181 [150] $\sigma_u$ , 553 [0] $\sigma_g$ , 395 [0] $\pi_g$ , 177 [2 $\times$ 0.6] $\pi_u$ ; $B_e = 1.5597$ ; $\mu = 0.004$
$\text{SC}_3\text{S}(\Sigma_g^+)$	2178 [3288] $\sigma_u$ , 1727 [0] $\sigma_g$ , 1038 [385] $\sigma_u$ , 502 [0] $\sigma_g$ , 412 [2 $\times$ 0] $\pi_g$ , 408 [2 $\times$ 1] $\pi_u$ , 86 [2 $\times$ 0.5] $\pi_u$ ; $B_e = 0.9133$ ; $\mu = 0$
$\text{SC}_4\text{S}(\Sigma_g^-)$	2139 [0] $\sigma_g$ , 1994 [925] $\sigma_u$ , 1417 [0] $\sigma_g$ , 884 [172] $\sigma_u$ , 441 [0] $\sigma_g$ , 398 [2 $\times$ 0.5] $\pi_u$ , 292 [2 $\times$ 0] $\pi_g$ , 226 [2 $\times$ 0] $\pi_g$ , 80 [2 $\times$ 0.05] $\pi_u$ ; $B_e = 0.576479$ ; $\mu = 0$
$\text{SC}_5\text{S}(\Sigma_g^+)$	2214 [6281] $\sigma_u$ , 2137 [0] $\sigma_g$ , 1738 [1744] $\sigma_u$ , 1280 [0] $\sigma_g$ , 808 [293] $\sigma_u$ , 425 [0] $\pi_g$ , 417 [2 $\times$ 1] $\pi_u$ , 405 [0] $\sigma_g$ , 267 [2 $\times$ 9] $\pi_u$ , 157 [0] $\pi_g$ , 21 [2 $\times$ 0.6] $\pi_u$ ; $B_e = 0.3957$ ; $\mu = 0.021$

<sup>a</sup> Experiment:  $B_0 = 6.47775$  GHz from ref 24. <sup>b</sup> Experiment:  $B_0 = 2.89038$  GHz from ref 17 and  $\mu = 3.704$  from ref 25. CCSD(T)-level computed harmonic vibrational frequencies are: 2100, 1536, 763, 482, 155  $\text{cm}^{-1}$  and  $\mu_e = 3.89$  D from ref 18. <sup>c</sup> Experiment:  $B_0 = 1.519165$  GHz from ref 11. <sup>d</sup> Experiment:  $B_0 = 0.9227$  GHz from ref 12. CEPA-1 level calculated harmonic vibrational frequencies are 2120, 2068, 1628, 1077, 537, 525, 455, 181, and 76  $\text{cm}^{-1}$  from ref 19.

**TABLE 3: Comparison of Experimental (Ar Matrix) and Calculated (B3LYP/6-311G\*) Most Intense IR Frequencies ( $\text{cm}^{-1}$ ) for Linear  $\text{C}_n\text{S}$  ( $n = 1-5$ ) and  $\text{SC}_n\text{S}$  ( $n=1-5$ ) Carbon–Sulfur Clusters in Their Electronic Ground States, and Relative Intensities (in Parentheses)**

$\text{C}_n\text{S}$ cluster	mode	$\nu_{\text{exp}}/\text{cm}^{-1}$	$\nu_{\text{cal}}^a/\text{cm}^{-1}$	$\text{SC}_n\text{S}$ cluster	mode	$\nu_{\text{exp}}/\text{cm}^{-1}$	$\nu_{\text{cal}}^a/\text{cm}^{-1}$
$\text{CS}(\Sigma^+)$	$\nu(\sigma)$ ; C–S	1275.1 <sup>b,c</sup>	1275.1	$\text{SCS}(\Sigma_g^+)$	$\nu(\sigma_u)$ ; C–S	1528.2(1.0) <sup>b,c</sup>	1540.6(1.0)
$\text{C}_2\text{S}(\Sigma^-)$	$\nu_1(\sigma)$ ; C–C		1652.1(1.0)	$\text{SC}_2\text{S}(\Sigma_g^-)$	$\nu_4(\sigma_u)$ ; C–S	1179.7(1.0) <sup>c</sup>	1157.4(1.0)
$\text{C}_3\text{S}(\Sigma^+)$	$\nu_1(\sigma)$ ; C–C	2047.6(1.0) <sup>b,d</sup>	2048.4(1.0)	$\text{SC}_3\text{S}(\Sigma_g^+)$	$\nu_3(\sigma_u)$ ; C–C	2078.5(1.0) <sup>b,c</sup>	2080.0(1.0)
	$\nu_2(\sigma)$ ; C–S	1533.7(0.1) <sup>d</sup>	1537.7(0.04)		$\nu_4(\sigma_u)$ ; C–S	1024.6(0.2) <sup>b,c</sup>	1017.2(0.12)
	$\nu_3(\sigma)$ ; C–S	725.6(0.009) <sup>d</sup>	724.2(0.009)				
$\text{C}_4\text{S}(\Sigma^-)$	$\nu_2(\sigma)$ ; C–C	1746.8(1.0) <sup>b</sup>	1728.6(1.0)	$\text{SC}_4\text{S}(\Sigma_g^-)$	$\nu_4(\sigma_u)$ ; C–C	1872.1(1.0) <sup>d</sup>	1856.5(1.0)
					$\nu_5(\sigma_u)$ ; C–S	897.7(0.117) <sup>d</sup>	866.3(0.19)
						843.7(0.056) <sup>d</sup>	
$\text{C}_5\text{S}(\Sigma^+)$	$\nu_1(\sigma)$ ; C–C	2124.5(1.0) <sup>b</sup>	2139.2(1.0)	$\text{SC}_5\text{S}(\Sigma_g^+)$	$\nu_4(\sigma_u)$ ; C–C	2104.7(1.0) <sup>d</sup>	2114.4(1.0)
	$\nu_3(\sigma)$ ; C–C		1581.5(0.15)		$\nu_5(\sigma_u)$ ; C–C	1687.9(0.36) <sup>d</sup>	1660(0.28)
					$\nu_6(\sigma_u)$ ; C–S	783.5(0.04) <sup>d</sup>	791.8(0.05)

<sup>a</sup> Scaled uniformly by 0.955 factor for modes with the C–C character mostly and by 0.980 factor for modes with the mostly C–S character. <sup>b</sup> Assignment proved based on the spectra recorded for the  $^{12/13}\text{C}$  substitution, this work. <sup>c</sup> Reference 9. <sup>d</sup> References 5–7.

**TABLE 4: Comparison of Experimental (Ar Matrix) and Calculated (MP2/6-31G\*, B3LYP/6-311G\* and CCSD(T) Levels) of Isotopic Shifts of  $\nu_1$  C–C Stretching Mode Frequencies ( $\text{cm}^{-1}$ ) for All Isotopomers of Linear  $^{12/13}\text{C}_3^{32}\text{S}$ , and Isotopic Shift Differences between Theoretical and Experimental Values (in Parentheses)**

isotopomer	expt	$\Delta_{\text{expt}}$	$\Delta_{\text{MP2}}^a$	$\Delta_{\text{B3LYP}}^b$	$\Delta_{\text{CCSD(T)}}^c$	$\Delta_{\text{CCSD(T)}}^d$
12–12–12–32	2047.6	0	0	0	0	0
13–12–12–32	2036.7	10.9	9.7	11.3	10.7	10.1
12–13–12–32	2001.0	46.6	45.5	48.1	48.5	47.0
12–12–13–32	2029.3	18.3	21.9	18.2	20.4	20.0
13–13–12–32	1990.4	57.2	54.9	59.1	59.1	59.1
13–12–13–32	2016.9	30.7	32.7	30.6	30.6	30.6
12–13–13–32	1981.0	66.6	69.2	70.3	70.3	70.3
13–13–13–32	1969.0	78.6	79.8	81.2	81.2	81.2

<sup>a</sup> Scaled by 0.9325 factor. <sup>b</sup> Scaled by 0.9545 factor. <sup>c</sup> Harmonic vibration wavenumbers from ref 18. <sup>d</sup> Anharmonic vibration wavenumbers from ref 18.

is smaller for the B3LYP/6-311G\* results than for MP2/6-31G\*. These deviations are higher though than for the pure carbon  $^{12/13}\text{C}_3$  clusters.

The isotopic shifts for the  $^{13}\text{CCC}^{32}\text{S}$ ,  $\text{C}^{13}\text{CC}^{32}\text{S}$ , and  $\text{CC}^{13}\text{C}^{32}\text{S}$  isotopomers, calculated by Seeger, Botschwina, et al.<sup>18</sup> from CCSD(T) theory, are also included in Table 4. All theoretical results quoted give similar results, with MP2 giving slightly larger deviations from experiment than the others. The assignment of the isotopomeric bands is unequivocal from all theories however.

Information on the mechanism of formation of the  $\text{C}_3\text{S}$  cluster can be gotten from the relative intensities of its isotopomeric bands. The intensities of the 2036.8  $\text{cm}^{-1}$  (13–12–12–32) and 2001.0  $\text{cm}^{-1}$  (12–13–12–32) bands are always found to have the same intensity, as shown in Figure 3. This has also been seen in other spectra using samples with different ( $^{12}\text{C}/^{13}\text{C}$ )

concentration ratios. This can be easily understood if  $\text{C}_3\text{S}$  is formed by the reaction of  $\text{C}_2$  with  $\text{CS}$ . For a given concentration of the reactants  $^{12}\text{C}^{13}\text{C}$  and  $^{12}\text{C}^{32}\text{S}$ , the above isotopomeric products would have an equal probability of formation. The energetically allowed reactions of  $\text{C}_3 + \text{S}$  are unlikely, because they involve the 13–12–12 and 12–13–12 isotopomers whose concentrations are different, as evidenced by the different intensities of the 2026.4 and 1987.7  $\text{cm}^{-1}$  bands (Figure 3). We can, however, not exclude the possible contribution of the  $\text{C} + \text{C}_2\text{S}$  reaction. Although this reaction is also highly exothermic (Figure 1), the relative concentration of the  $\text{C}_2\text{S}$  isotopomers was impossible to track, due to their low intensities. The most intense  $\text{C}_2\text{S}$  vibration is calculated to be only 42  $\text{km/mol}$ .

**$\text{C}_4\text{S}$  Cluster.** The 1746.8  $\text{cm}^{-1}$  band is assigned here to the linear  $\text{C}_4\text{S}$  cluster. This band, shown in Figure 2b from a  $^{12}\text{C}/^{32}\text{S}$  run, is as intense as the 1275.1  $\text{cm}^{-1}$  band attributed to  $\text{CS}$ .

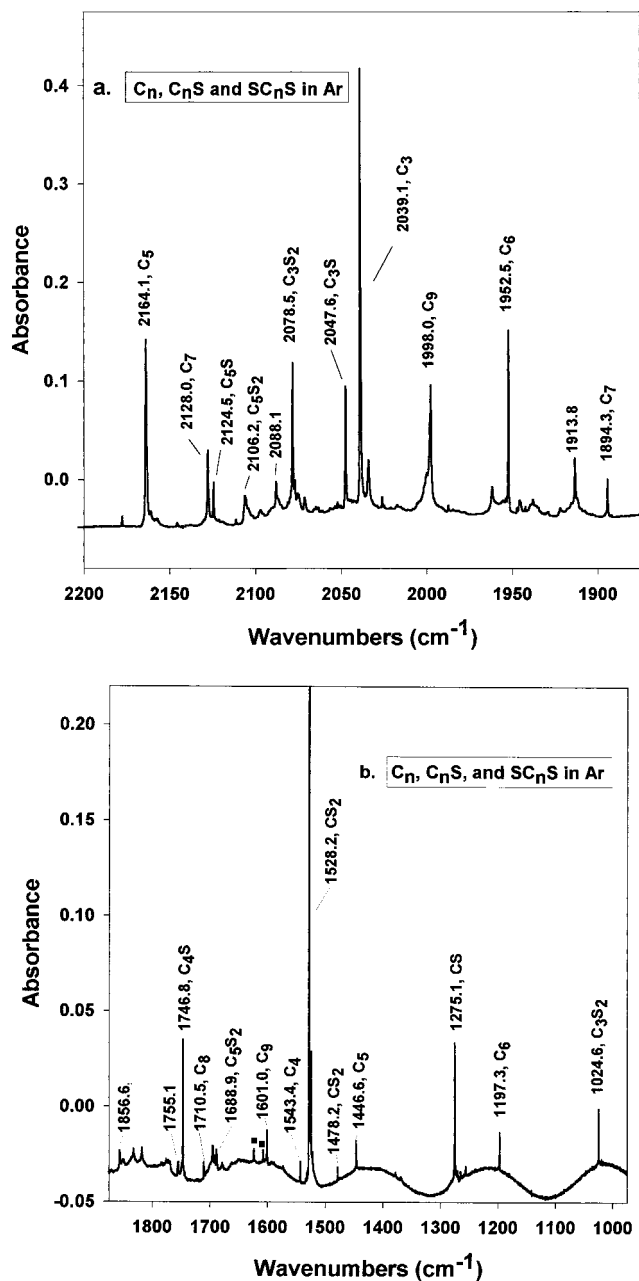


**Figure 2.** Overview infrared absorption spectrum in two energy regions after Ar matrix deposition of products from the laser-ablation of a mixture of graphite (98.9%  $^{12}C$  + 1.1%  $^{13}C$ ) and sulfur (96%  $^{32}S$  + 4%  $^{34}S$ ). Products are marked in the spectrum. Bands indicated by squares are due to isolated  $H_2O$  molecules. The 1478.2  $cm^{-1}$  band is due to the  $^{13}C^{32}S_2$  isotopomer.

Calculations predict a band for  $C_4S$  at 1810  $cm^{-1}$  (unscaled)/1728.6  $cm^{-1}$  (scaled) (Tables 2 and 3). While these results are strongly suggestive of a  $C_4S$  assignment, isotopic substitution studies unambiguously confirm this choice. The spectra in Figure 4 show the use of a 6-fold higher concentration of  $^{12}C$  vs  $^{13}C$  (upper spectrum) and the reverse isotopic ratio (lower spectrum). A 6:1 concentration ratio ensures the formation of either all- $^{12}C$  or singly- $^{13}C$ -substituted isotopomers, and vice versa. Use of an equimolar ratio of  $^{12}C$  and  $^{13}C$  isotopes results in the spectrum shown in Figure 5 (upper spectrum). Sixteen bands are observed. The bands due to clusters with higher numbers of  $^{13}C$  atoms are more intense. This may be explained by the fact that the  $^{13}C$  material is less cohesive than  $^{12}C$  and thus easier to ablate.

The observed 16 isotopomeric peaks strongly point to the

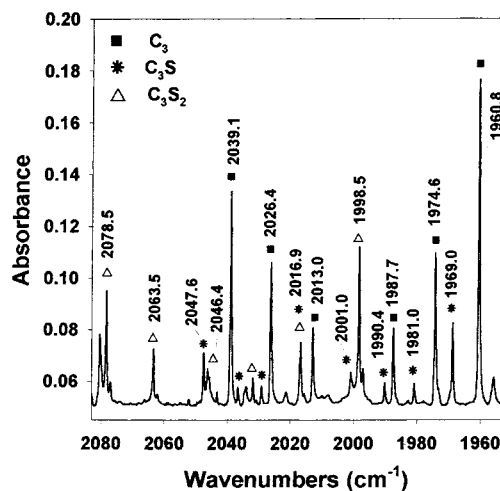


**Figure 3.** Absorption spectrum of  $^{12/13}C_3$ ,  $^{12/13}C_3^{32}S$ , and  $^{12/13}C_3^{32}S_2$  species isolated in an Ar matrix at 12 K in the C–C stretching vibration region. All isotopomeric bands are marked. The 2080.5 and 2045.8  $cm^{-1}$  bands (not marked) are due to  $^{13}C_5$  and  $^{13}C_7$  isotopomers, respectively. The low-intensity, broad bands (not marked) 4.8  $cm^{-1}$  red-shifted from the  $^{12/13}C_3$  isotopomer peaks are due to  $^{12/13}C_3$  isotopomers trapped in a secondary site in the Ar matrix. The carrier of the 2043.4  $cm^{-1}$  band (not marked) is  $^{13}C_3^{32}S$  isotopomer.

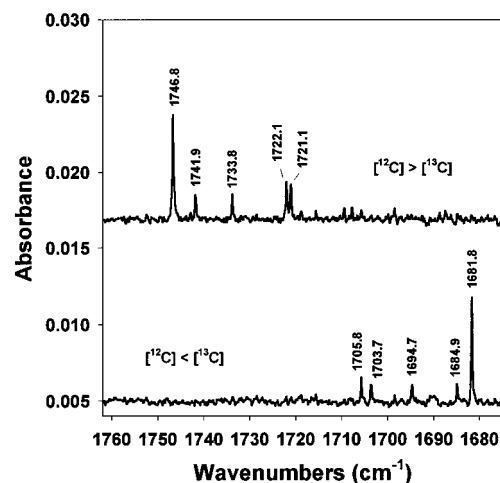


**Figure 4.** IR absorption spectra of  $^{12/13}C_4^{32}S$  clusters isolated in solid Ar at 12 K. The upper spectrum was recorded on a sample/matrix prepared using a  $[^{12}C]/[^{13}C] = 6$  concentration ratio, while in the lower spectrum  $[^{13}C]/[^{12}C] = 6$ . The bands marked are due to isotopomers with either all- $^{12}C$  or singly- $^{13}C$ -substituted  $C_4S$  clusters (upper spectrum) or all- $^{13}C$  and singly- $^{12}C$ -substituted isotopomers (lower spectrum).

carrier of these bands as linear  $C_4S$ , for which 16 bands are expected. Comparison with the predicted isotopic band pattern confirms this. The isotopic band frequencies for linear  $^{12/13}C_4^{32}S$  clusters, calculated at the MP2/6-31G\* and B3LYP/6-311G\* levels, are collected in Table 5. The predicted pattern is very similar to the experimental one. Although the comparison (using the same level of theory) is worse than for pure  $^{12/13}C_4$  clusters, it is sufficiently close to lead to the conclusion that the 1746.8  $cm^{-1}$  band arises from the linear  $C_4S$  cluster.

Information on the mechanism of formation of  $C_4S$  may be deduced from observed isotopomeric band intensities. For all experiments with different  $^{12}C$  to  $^{13}C$  concentration ratios, the intensity of the 1741.9  $cm^{-1}$  (12–12–13–12–32) band is the same as for the 1733.8  $cm^{-1}$  (13–12–12–12–32) band. The same situation exists for the 1694.7  $cm^{-1}$  (12–13–13–13–32) and 1684.9  $cm^{-1}$  (13–13–12–13–32) pair and the 1715.7

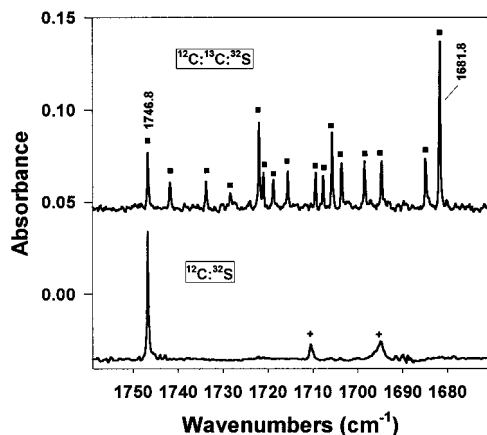


**Figure 5.** IR absorption spectra of C–C stretching vibration in  $^{12/13}\text{C}_4\text{S}$  clusters (upper spectrum) and in the  $^{12}\text{C}_4\text{S}$  cluster (lower spectrum) isolated in Ar at 12 K. All 16 isotopomers for  $\text{C}_4\text{S}$  are marked by squares. The crossed bands located at 1710.5 and 1695  $\text{cm}^{-1}$  in the lower spectrum are due to larger “pure” carbon clusters.

**TABLE 5: Observed (Ar Matrix) and Calculated (MP2/6-31G\* and B3LYP/6-311G\*)  $\nu_3$  C–C Stretching Mode Frequencies ( $\text{cm}^{-1}$ ) for All Isotopomers of Linear  $^{12/13}\text{C}_4\text{S}_2$**

isotopomer	expt	MP2 <sup>a</sup>	$\Delta\text{MP2}$	B3LYP <sup>b</sup>	$\Delta\text{B3LYP}$
12–12–12–12–32	1746.8	1746.8	0	1746.8	0
13–12–12–12–32	1733.8	1734.4	0.6	1734.2	0.4
12–13–12–12–32	1721.1	1718.9	–2.2	1718.7	–2.4
12–12–13–12–32	1741.9	1743.2	1.3	1743.2	1.3
12–12–12–13–32	1722.1	1721.1	–1.0	1721.4	–0.7
13–13–12–12–32	1707.8	1705.4	–2.4	1705.1	–2.7
12–13–13–12–32	1718.9	1717.3	–1.6	1717.1	–1.8
12–12–13–13–32	1715.7	1715.1	–0.6	1715.5	0.2
13–12–13–12–32	1728.5	1731.5	3.0	1731.5	3.0
13–12–12–13–32	1709.4	1708.4	–1.0	1708.7	–0.7
12–13–12–13–32	1698.5	1696.1	–2.4	1696.0	–2.5
13–13–13–12–32	1705.8	1704.3	–1.5	1703.9	–1.9
13–13–12–13–32	1684.9	1682.2	–2.7	1682.1	–2.8
13–12–13–13–32	1703.7	1703.4	–0.3	1703.7	0.0
12–13–13–13–32	1694.7	1692.6	–2.1	1692.6	–2.1
13–13–13–13–32	1681.8	1679.4	–2.4	1679.3	–2.5

<sup>a</sup> Scaled by 0.9619 factor. <sup>b</sup> Scaled by 0.9652 factor.

$\text{cm}^{-1}$  (12–12–13–13–32) and 1709.4  $\text{cm}^{-1}$  (13–12–12–13–32) pair (cf. Figures 4 and 5). This unique intensity band pattern can be understood if the mechanism of  $\text{C}_4\text{S}$  cluster formation involves the reaction between  $^{12/13}\text{C}_3$  and  $^{12/13}\text{C}_3^{32}\text{S}$  isotopomers. In each pair of  $\text{C}_4\text{S}$  products above, only the  $^{12/13}\text{C}_3$  and  $^{12/13}\text{C}_3^{32}\text{S}$  species would lead to the equal intensity product bands found. All other possible reactants which might form equal intensity bands have isotopomeric bands which display different concentrations. All, that is, except the  $\text{C}_2$  and  $\text{C}_2\text{S}$  reactants for which no IR absorption was observed. The  $\text{C}_2 + \text{C}_2\text{S}$  reaction is calculated to be the most exothermic of all the carbon cluster + carbon–sulfur cluster reactions (Figure 1). It could contribute to the production of  $\text{C}_4\text{S}$ .

In Figure 5 (upper), the 1703.7  $\text{cm}^{-1}$  (13–12–13–13–32) band has the same intensity as the 1698.5  $\text{cm}^{-1}$  (12–13–12–13–32) band, even though the 13–12–13 and 12–13–12 clusters are different. But Figure 3 (which is from the same run as Figure 5, upper spectrum) shows that the 13–12–13 and 12–13–12 isotopomer bands, located at 2013 and 1987.7  $\text{cm}^{-1}$ , respectively, have the same intensities. Thus, it is expected that if these  $\text{C}_3$  isotopomers react with the  $^{13}\text{C}_3^{32}\text{S}$  species the product isotopomers, 13–12–13–13–32 and 12–13–12–13–32, should have the same band intensities. This is found experimentally.

The  $\text{C}_3 + \text{CS} \rightarrow \text{C}_4\text{S}$  reaction is favored by the fact that the relative concentration of  $\text{C}_3$  in the matrix is large and the small

**TABLE 6: Comparison of Observed (Ar Matrix, 12 K) and Calculated (B3LYP/6-311G\*) Isotopomer Frequencies ( $\text{cm}^{-1}$ ) for All- $^{12}\text{C}$ , Singly- $^{13}\text{C}$ , or  $^{12}\text{C}$  Substituted and All- $^{13}\text{C}$  Substituted  $^{12/13}\text{C}_5^{32}\text{S}$  Linear Carbon–Sulfur Clusters**

isotopomer	$\nu_{\text{exp}}$	$\Delta\nu_{\text{exp}}$	$\nu_{\text{B3LYP}}^a$	$\Delta\nu_{\text{B3LYP}}$	$\nu_{\text{exp}} - \nu_{\text{B3LYP}}$
12–12–12–12–12–32	2124.5	0	2124.5	0	0
13–12–12–12–12–32	2123.8	0.7	2123.0	1.5	0.8
12–12–12–12–13–32	2120.3	4.2	2120.8	3.7	–0.5
12–13–12–12–12–32	2114.4	10.1	2113.3	11.2	1.1
12–12–12–13–12–32	2101.4	23.1	2099.8	24.7	1.6
12–12–13–12–12–32	~2091.3 <sup>b</sup>	33.2	2091.8	32.7	–0.5
13–13–12–13–13–32	~2078.5 <sup>c</sup>	46.0	2077.2	47.3	1.3
13–13–13–12–13–32	2075.6	48.9	2074.1	50.4	1.5
13–12–13–13–13–32	~2058.8 <sup>d</sup>	65.7	2059.1	65.4	–0.3
13–13–13–13–12–32	2048.8	75.7	2046.4	78.1	2.4
12–13–13–13–13–32	~2045.8 <sup>e</sup>	78.7	2043.0	81.5	2.8
13–13–13–13–13–32	2043.4	81.1	2041.2	83.3	2.2

<sup>a</sup> Scaled by 0.9484 factor. <sup>b</sup> Overlapped with the  $^{13}\text{C}^{16}\text{O}$  band. <sup>c</sup> Covered by the 2078.5  $\text{cm}^{-1}$  ( $^{12}\text{C}_3^{32}\text{S}_2$ ) strong band. <sup>d</sup> Overlapped with the 2058.7  $\text{cm}^{-1}$  band due to  $^{12/13}\text{C}_7$  isotopomer. <sup>e</sup> Blended with the 2045.8  $\text{cm}^{-1}$  ( $^{13}\text{C}_7$ ) strong band.

$\text{CS}$  species is known to be mobile in the matrix.<sup>9</sup> This mobility is reflected by the observation here of the van der Waals complex,  $(\text{CS})_2$ , formed during matrix annealing. In fact, all isotopomeric bands of  $\text{C}_4\text{S}$  grow substantially during matrix annealing, while the  $^{12/13}\text{CS}$  bands decline in intensity but at a much slower rate. This results from the regeneration of  $\text{CS}$  via the  $\text{C} + \text{S}$  reaction. All the above observations support the mechanism of  $\text{C}_4\text{S}$  formation occurring mainly via the  $\text{C}_3 + \text{CS}$  reaction with a minor route possibly via the  $\text{C}_2 + \text{C}_2\text{S}$  reaction.

Finally, the 1757  $\text{cm}^{-1}$  absorption (Ar matrix), attributed<sup>6</sup> to  $\text{C}_4\text{S}$ , one of many pyrolysis products of cyclic precursors (containing C, S, and O), is not observed in our spectra. Its assignment to  $\text{C}_4\text{S}$  is therefore questionable.

**$\text{C}_5\text{S}$  Cluster.** In agreement with earlier CEPA-1 calculations by Botschwina et al.<sup>19</sup> and DFT calculations by Lee,<sup>20</sup> our B3LYP/6-311G\* calculations predict that  $\text{C}_5\text{S}$  should have an intense C–C stretching vibration, which in our work falls at 2139  $\text{cm}^{-1}$  (0.955 scale factor), with an integral intensity of almost 4000  $\text{km/mol}$  (Table 3). Search for a band in this region revealed a strong band at 2124.5  $\text{cm}^{-1}$ . Using  $^{13}\text{C}/\text{S}$  ablation mixtures shifts the band to 2043.4  $\text{cm}^{-1}$  (Figure 3), leading to its assignment to the  $^{13}\text{C}_5^{32}\text{S}$  isotopomer. To prove the origin of these bands, mixed isotopic substitution is very informative.  $^{12/13}\text{C}/\text{S}$  mixtures, with  $[\text{C}^{12}]/[\text{C}^{13}] = 6$  and the reverse isotopic ratios, were laser ablated. For the  $[\text{C}^{12}]/[\text{C}^{13}] = 6$  sample, the observed bands are expected to be due to either all- $^{12}\text{C}$  or singly- $^{13}\text{C}$  substituted isotopomers whereas either all- $^{13}\text{C}$  or singly- $^{12}\text{C}$  substituted isotopomers are expected for the  $[\text{C}^{13}]/[\text{C}^{12}] = 6$  sample. This expectation is consistent with the patterns observed here for the  $\text{C}_3\text{S}$ ,  $\text{C}_3\text{S}_2$ ,  $\text{C}_4\text{S}$ , and all  $\text{C}_n$  clusters. The experimental band patterns bounded by the 2124.5 and 2043.4  $\text{cm}^{-1}$  bands are listed in Table 6, along with a comparison to calculated (MP2/6-31G\* and B3LYP/6-311G\*) values. The experimental band positions fit reasonably well with the predicted frequencies. The largest discrepancy between experiment and theory is 2.8  $\text{cm}^{-1}$  for the 12–13–13–13–13–32 isotopomer. However, this band is overlapped with the strong  $^{13}\text{C}_7$  band at 2045.8  $\text{cm}^{-1}$  and is thus uncertain by ca. 1  $\text{cm}^{-1}$ . From  $[\text{C}^{13}]/[\text{C}^{12}] = 6$  mixtures, it is found that many singly- $^{12}\text{C}$  substituted isotopomers of  $\text{C}_5\text{S}$  overlap with  $\text{C}_3\text{S}_2$  and  $\text{C}_7$  isotopomeric bands. Table 6 indicates the overlap. For this reason the precise position of these bands is tentative. In conclusion, based on the good agreement between observed and

calculated band positions for singly- $^{13}\text{C}$  substituted isotopomers of  $^{12/13}\text{C}_5^{32}\text{S}$ , we assign the  $2124.5\text{ cm}^{-1}$  absorption to the linear $^{12}\text{C}_5^{32}\text{S}$  cluster.

**Other Small Clusters.** In addition to the carbon–sulfur species discussed above, there are several others listed in Table 3 which merit comment.

A full isotopic study ( $^{12,13}\text{C},^{32,34}\text{S}$ ) was first reported by Andrews et al.<sup>9</sup> for CS. But interestingly, the next species in the series,  $\text{C}_2\text{S}$ , has not yet been observed, presumably due to its low expected intensity. Our DFT-calculated vibrational frequency is predicted to fall at  $1652.1\text{ cm}^{-1}$ . The  $\text{CS}_2$  species is, of course, the analogue of  $\text{CO}_2$  and exhibits a well-known<sup>9</sup> strong band at  $1528.2\text{ cm}^{-1}$ . The asymmetric CS stretch in  $\text{C}_2\text{S}_2$  at  $1179.7\text{ cm}^{-1}$  has been thoroughly studied via isotopic substitution by Andrews and co-workers.<sup>9</sup> The CC stretching frequency ( $1904\text{ cm}^{-1}$ ) in  $\text{C}_2\text{S}_2$  was reported by Maier and co-workers.<sup>8</sup>

Of the remaining larger species,  $\text{C}_3\text{S}_2$ ,  $\text{C}_4\text{S}_2$ , and  $\text{C}_5\text{S}_2$ , only  $\text{C}_3\text{S}_2$  has been studied via isotopic substitution. Maier et al. reported<sup>7</sup> the experimental  $\text{C}_3\text{S}_2$  frequencies first and included results from PM3 calculations. The vibrational positions found, with the theoretical values (given in parentheses), are  $2078.4$  ( $2225\text{ cm}^{-1}$ ),  $1024.5$  ( $961\text{ cm}^{-1}$ ),  $465$  ( $669\text{ cm}^{-1}$ ), and  $107$  ( $127\text{ cm}^{-1}$ ). Later, Andrews et al.,<sup>9</sup> using an electrical discharge through isotopic mixtures of  $\text{CS}_2$  and Ar, provided strong evidence for  $\text{C}_3\text{S}_2$  modes at  $2078.6$  and  $1024.1\text{ cm}^{-1}$ . In the present work, bands attributable to  $\text{C}_3\text{S}_2$  were found at  $2078.5$  and  $1024.6\text{ cm}^{-1}$ , which also match well with the calculated DFT positions at  $2080.0$  and  $1017.2\text{ cm}^{-1}$ .

Maier and co-workers have presented evidence<sup>5</sup> for bands at  $1872.1$ ,  $897.7$ , and  $843.7\text{ cm}^{-1}$  attributable to  $\text{C}_4\text{S}_2$ , which agree reasonably well with the present computed values of  $1856.5$  and  $866.3\text{ cm}^{-1}$ .

Finally, the reported<sup>7</sup> values for the symmetrical  $\text{C}_5\text{S}_2$  species at  $2104.7$ ,  $1687.9$ , and  $783.5$  match closely with the computed values found here at  $2114.4$ ,  $1660$ , and  $791.8\text{ cm}^{-1}$ .

#### IV. Possible Astrophysical Implications

The estimated column density for  $\text{C}_3\text{S}$  in the circumstellar envelope of IRC+10216 is roughly 25 times smaller than for  $\text{C}_3$ .<sup>3</sup> The B3LYP/6-311G\*-calculated intensity of the most intense IR absorption in  $\text{C}_3\text{S}$  is twice that in  $\text{C}_3$ . This suggests that the infrared signal resulting from the C–C vibration in  $\text{C}_3\text{S}$  should be observable from the IRC+10216. It should be only 12.5 times smaller than the signal reported for  $\text{C}_3$ .

The estimated column density for the  $\text{C}_5$  cluster, which has been identified by direct IR observation of IRC+10216,<sup>22</sup> is twice that for  $\text{C}_5\text{S}$ ,<sup>3</sup> but the intensity of the calculated  $2240\text{ cm}^{-1}$  band of  $\text{C}_5\text{S}$  is 1.5 times higher than for the most intense mode of  $\text{C}_5$ , and only 0.6 times lower than for  $\text{C}_5\text{S}_2$ . This leads to the conclusion that direct IR observation of  $\text{C}_5\text{S}$  and  $\text{C}_5\text{S}_2$  in IRC+10216 should be feasible (assuming that the  $\text{C}_5\text{S}$  and  $\text{C}_5\text{S}_2$  clusters have similar column densities). This is an attractive proposition, particularly for the  $\text{C}_n\text{S}_2$  clusters which are silent in radioastronomy observations due to their lack of a permanent electric dipole moment.

To explain the chemistry of  $\text{C}_n\text{S}$  clusters in the interstellar space, many reaction models have previously been proposed, most of which assume that the  $\text{S}^+$  ion plays a major role.<sup>27–29</sup> Such an ion is not expected to be present in the experiments reported here. The laser ablation used a relatively low flux of laser photons which produced no plasma at the vaporization point. Under these experimental conditions the ion-to-neutral concentration ratio is expected to be very low. The average

electron current collected by a  $+100\text{ V}$  electrode located  $3\text{ cm}$  from the vaporization spot was lower than  $1\text{ }\mu\text{A}$ . This current also includes the secondary electrons released by electron impact ionization processes in Ar. Finally, in the IR spectra recorded here no bands due to any ionic  $\text{C}_n^+$  species were observed.<sup>30</sup> Thus, neutral–neutral reactions rather than reactions involving  $\text{S}^+$  are believed to be far more important in the production of the  $\text{C}_n\text{S}$  and  $\text{SC}_n\text{S}$  clusters studied here.

These neutral–neutral reactions could be important in that portion of interstellar space from which carbon atoms, carbon clusters, sulfur atoms, and carbon–sulfur clusters have been observed, such as IRC+10216 and TMC-1.  $\text{C}_n\text{S}$  and  $\text{SC}_n\text{S}$  species could be formed in the gas phase as well as on the surface of cold ice mantles of dust grains in space.

#### V. Conclusions

Employing FT-IR absorption spectroscopic methods with density functional calculations, the  $^{12/13}\text{C}_4^{32}\text{S}$  and  $^{12/13}\text{C}_5^{32}\text{S}$  linear carbon–sulfur clusters have been identified in Ar matrices at  $12\text{ K}$ . In particular, the  $1746.8$  and  $2124.5\text{ cm}^{-1}$  absorption bands have been assigned to the  $\nu_2$  and  $\nu_1$  C–C stretching modes of  $^{12}\text{C}_4^{32}\text{S}$  and  $^{12}\text{C}_5^{32}\text{S}$ , respectively.

The mechanism of  $\text{C}_4\text{S}$  formation in the matrix most likely involves the reaction of  $\text{C}_3 + \text{CS}$ . The reaction of  $\text{C}_2 + \text{C}_2\text{S}$  cannot be ruled out, but is considered less likely.

The mechanism of formation of  $\text{C}_n\text{S}$  and  $\text{SC}_n\text{S}$  clusters in interstellar space may involve neutral–neutral type reactions on the surface of cold ice mantles of dust grains.

**Acknowledgment.** The authors gratefully acknowledge the National Aeronautics and Space Administration and the Petroleum Research Foundation, administered by the American Chemical Society, for their support of this research.

#### References and Notes

- (1) Cernicharo, J.; Guelin, M.; Hein, H.; Kahane, C. *Astron. Astrophys.* **1987a**, *181*, L119.
- (2) Yamamoto, S.; Saito, S.; Kawaguchi, K.; Kaifu, N.; Suzuki, H.; Ohishi, M. *Astrophys. J.* **1987**, *317*, L119.
- (3) Bell, M. B.; Avery, L. W.; Feldman, P. A. *Astrophys. J.* **1993**, *417*, L37–L40.
- (4) Spiro, C. L.; Banholtzer, W. F.; McAtee, D. S. *Thin Solid Films* **1992**, *220*, 122.
- (5) Maier, G.; Schrot, J.; Reisenauer, H. P.; Janoschek, R. *Chem. Ber.* **1991**, *124*, 2617. The  $2046.2\text{ cm}^{-1}$  value reported for  $\text{C}_3\text{S}$  in Ar is  $1.4\text{ cm}^{-1}$  lower than our value.
- (6) Maier, G.; Schrot, J.; Reisenauer, H. P. *Chem. Ber.* **1991**, *124*, 2613.
- (7) Maier, G.; Schrot, J.; Reisenauer, H. P.; Janoschek, R. *Chem. Ber.* **1990**, *123*, 1753.
- (8) Maier, G.; Reisenauer, H. P.; Schrot, J.; Janoschek, R. *Angew. Chem., Int. Ed. Engl.* **1990**, *29*, 1464.
- (9) Bohn, R. B.; Hannachi, Y.; Andrews, L. *J. Am. Chem. Soc.* **1992**, *114*, 6452.
- (10) Ohshima, Y.; Endo, Y. *J. Mol. Spectrosc.* **1992**, *153*, 627.
- (11) Hirahara, Y.; Ohshima, Y.; Endo, Y. *Astrophys. J.* **1993**, *408*, L113–L115.
- (12) Kasai, Y.; Obi, K.; Ohshima, Y.; Hirahara, Y.; Endo, Y.; Kawaguchi, K.; Murakami, A. *Astrophys. J.* **1993**, *410*, L45–L47.
- (13) Sulze, D.; Beye, N.; Fanghanel, E.; Schwarz, H. *Chem. Ber.* **1990**, *123*, 2069.
- (14) Peeso, D. J.; Ewing, D. W.; Curtis, T. T. *Chem. Phys. Lett.* **1990**, *166*, 307.
- (15) Maurakami, A., *Astrophys. J.* **1990**, *357*, 288.
- (16) Y. Zie; Schaefer III, H. F. *J. Chem. Phys.* **1992**, *96*, 3714.
- (17) Cai, Z. L.; Zhang, X. G.; Wang, X. Y. *Chem. Phys. Lett.* **1990**, *213*, 168.
- (18) Seeger, S.; Botschwina, P.; Flugge, J.; Reisenauer, H. P.; Maier, G. *J. Mol. Struct.* **1994**, *303*, 213.
- (19) Seeger, S.; Flugge, J.; Botschwina, P. Poster P/I-107, 8th International Congress of Quantum Chemistry, Prague, June 19–23, **1994**. Botschwina, P., private communication.
- (20) Lee, S. *Chem. Phys. Lett.* **1997**, *268*, 69.

(21) Frisch, M. J.; Trucks, G. W.; Schlegel, H. B.; Gill, P. M.; Johnson, B. G.; Robb, M. R.; Cheeseman, J. R.; Keith, T. A.; Peterson, G. A.; Montgomery, J. A.; Raghavachari, K.; Al-Laham, M. A.; Zakrzewski, V. J.; Ortiz, J. V.; Foresman, J. B.; Cioslowski, J.; Stefanov, B. B.; Nanayakkara, A.; Challacombe, M.; Peng, C. Y.; Ayala, P. Y.; Chen, W.; Wong, M. W.; Andres, J. L.; Replogle, E. S.; Gomperts, R.; Martin, R. L.; Fox, D. J.; Binkley, J. S.; Defrees, D. J.; Baker, J.; Stewart, J. P.; Head-Gordon, M.; Gonzalez, C.; Pople, J. A. *GAUSSIAN 94*, Revision B.2; Gaussian, Inc.: Pittsburgh, PA, 1995.

(22) Bernath, P.; Hinkle, K.; Keady, J. *Science* **1989**, *244*, 562.

(23) Van Orden, A.; Saykally, R. *Chem. Rev.* **1998**, *98*, 2313.

(24) Yamamoto, S.; Saito, S.; Kawaguchi, K.; Chicada, Y.; Suzuki, H.; Kaifu, N.; Ishikawa, S. *Astrophys. J.* **1990**, *361*, 318.

(25) Suenram, R. D.; Lovas, F. J. *Astrophys. J.* **1994**, *429*, L89.

(26) Bogey, M.; Demuyneck, C.; Destombes, J. L. *J. Mol. Spectrosc.* **1982**, *95*, 35.

(27) Prasad, S. S.; Huntress, W. T. Jr. *Astrophys. J.* **1982**, *260*, 590.

(28) Smith, D.; Adams, N. G.; Giles, K.; Herbst, E. *Astronom. Astrophys.* **1988**, *200*, 191.

(29) Miller, T. J.; Herbert, E. *Astronom. Astrophys.* **1990**, *231*, 466.

(30) Szczepanski, J.; Hodyss, R.; Vala, M. *J. Phys. Chem.* **1998**, *102*, 8300.